

AperTO - Archivio Istituzionale Open Access dell'Università di Torino

**MODIS-derived EVI, NDVI and WDRVI time series to estimate phenological metrics in French deciduous forests**

**This is the author's manuscript**

*Original Citation:*

*Availability:*

This version is available <http://hdl.handle.net/2318/1648576> since 2022-06-01T15:09:43Z

*Published version:*

DOI:10.1016/j.jag.2017.08.006

*Terms of use:*

Open Access

Anyone can freely access the full text of works made available as "Open Access". Works made available under a Creative Commons license can be used according to the terms and conditions of said license. Use of all other works requires consent of the right holder (author or publisher) if not exempted from copyright protection by the applicable law.

(Article begins on next page)

# MODIS-derived EVI, NDVI and WDRVI time series to estimate phenological metrics in French deciduous forests

S. Testa<sup>1\*</sup>, K. Soudani<sup>2</sup>, L. Boschetti<sup>3</sup>, E. Borgogno Mondino<sup>1</sup>

1: Department of Agricultural, Forest and Food Sciences, University of Turin, Grugliasco (TO), Italy.

2: Univ. Paris-Sud, Laboratoire Ecologie Systématique et Evolution, UMR8079, F-91405. CNRS, Orsay, France.

3: Department of Forest, Rangeland, and Fire Sciences, University of Idaho, Moscow, ID (USA)

\*Corresponding author: stefano.testa@hotmail.com

## Abstract

Monitoring forest phenology allows us to study the effects of climate change on vegetated land surfaces. Daily and composite time series (TS) of several vegetation indices (VIs) from MODerate resolution Imaging Spectroradiometer (MODIS) data have been widely used in scientific works for phenological studies since the beginning of the MODIS mission. The objective of this work was to use MODIS data to find the best VI/TS combination to estimate start-of-season (SOS) and end-of-season (EOS) dates across 50 temperate deciduous forests. Our research used as inputs 2001-2012 daily reflectance from MOD09GQ/MOD09GA products and 16-day composite VIs from the MOD13Q1 dataset. The 50 pixels centered on the 50 forest plots were extracted from the above-mentioned MODIS imagery; we then generated 5 different types of TS (1 daily from MOD09 and 4 composite from MOD13Q1) and used all of them to implement 6 VIs, obtaining 30 VI/TS combinations. SOS and EOS estimates were determined for each pixel/year and each VI/TS combination. SOS/EOS estimations were then validated against ground phenological observations. Results showed that, in our test areas, composite TS, if actual acquisition date is considered, performed mostly better than daily TS. EVI, WDRVI<sub>0.20</sub> and NDVI were more suitable to SOS estimation, while WDRVI<sub>0.05</sub> and EVI were more convenient in estimating early and advanced EOS, respectively.

**Keywords:** Forest phenology; MODIS time series; EVI; WDRVI; NDVI

## 1 – Introduction

The concept of phenology was initially introduced by Morren (1849) as “the science having the goal to understand the manifestations of life governed by time” (Demarée and Rutishauser 2009). Phenology is currently defined by

1 the United States International Biological Program Committee as the study of (a) the timing of recurring  
2 biological events; (b) the causes of their timing with regard to biotic and abiotic forces; and, (c) the interrelation  
3 among phases of the same or different species (Lieth 1974). Surveying forest phenology requires the observation  
4 of the timing of events such as bud burst, and leaves emerging, developing and falling (Liang and Schwartz 2009;  
5 Nordli et al. 2008; Richardson et al. 2013; Thomas et al. 2010).

6 Adopting the terminology commonly used in previous studies, phenological stages are defined as the  
7 developmental stages of an organism's life cycle (Ruml and Vulić 2005); the corresponding measurement is the  
8 date of occurrence, i.e. the date in which the phenological stage is first observed. Phenological phases are defined  
9 as the time interval between the date of occurrence of two consecutive phenological stages (Ruml and Vulić  
10 2005).

11 Accurate long-term monitoring of plant phenology at global and continental scales allows the evaluation of the  
12 interactions and feedback between climate and vegetation (Bradley et al. 1999; Fabian and Menzel 1998; Koch et  
13 al. 2008; Richardson et al. 2013; Schwartz 1998). Vegetation phenology is responsive to environmental and  
14 climatic dynamics (Crucifix et al. 2005; Penuelas and Filella 2001), but also influences them (Penuelas et al.  
15 2009; Richardson et al. 2013), with repercussions on water and biogeochemical cycles (Cowie 2007; Gu et al.  
16 2003; Noormets 2009). At the single-plant or stand scale, vegetation phenology is affected by individuals' traits  
17 (genes, age), soil (temperature, nutrients, flora, fauna, wetness), pests, diseases, intra- and extra-specific  
18 competition, micro-climate, water availability, pollinators and other factors (Defila 1992; Elzinga et al. 2007;  
19 Fenner 1998). At the macro-scale, temperature (Brooke et al. 1996), photoperiod (Vitasse and Basler 2013) and  
20 precipitation (Lieberman and Milton 1984) are the main phenological drivers (Fenner 1998; Keatley and Fletcher  
21 2003; Sarvas 1972, 1974), that are affected in turn by the biome and its vegetation.

22 Numerous phenological studies found earlier onset of plant growth and longer vegetative season at mid and high  
23 latitudes in the northern hemisphere (European Environment Agency 2004, 2012; Koch et al. 2008; Menzel and  
24 Fabian 1999; Nordli et al. 2008; Parmesan and Galbraith 2004; Rosenzweig et al. 2007; Schaber and Badeck  
25 2005; Henebry 2013).

26 Other phenological studies demonstrated that phenological stages in temperate forests begin and totally develop in  
27 7 to 33 days (Aubinet et al. 2002; Bequet et al. 2011; Breda et al. 1995; Brügger et al. 2003; Gond et al. 1999;  
28 Granier et al. 2000; Soudani et al. 2012). A review of phenological trends is available in Richardson et al. (2013).

1 Remote sensing is a key instrument in global monitoring (Reed et al. 2003) in that a number of satellite missions  
2 guarantee repeated, periodic observations of the Earth's entire surface from a very unique point of view. In fact,  
3 satellites provide near-global observations of the climate system, and they are playing a major role in global  
4 climate observing (World Meteorological Organization 2006). Ongoing climate change sets an important  
5 objective for the remote sensing phenology-oriented scientific community: to estimate the timing of phenological  
6 stages accurately and precisely enough to remedy the lack of ground surveys. Field measurements will always be  
7 essential to validate estimates based on space data (Beaubien and Hall-Beyer 2003), despite the issue of the  
8 different reference scale (a "point" in ground surveys, an area in satellite acquisitions) (Morissette et al. 2009).

9 Land surface phenology (LSP) monitoring from satellite data relies on the availability of large series of consistent,  
10 spatially coincident observations, and it is mostly conducted through time series (TS) analysis (Ahl et al. 2006;  
11 Bradley et al. 2007; Busetto et al. 2010; Colombo et al. 2011; Colombo et al. 2009; de Beurs and Henebry 2004;  
12 Gutman et al. 1995; Jönsson and Eklundh 2002; Jönsson and Eklundh 2003). Typically, satellite data are  
13 preprocessed by applying a fitting/smoothing algorithm, and then a set of criteria is applied to estimate the timing  
14 of the phenological stages. When considering temporal trends in phenological metrics, attention should be paid to  
15 their reliable detection (de Beurs and Henebry 2005).

16 Among the available RS data, NASA's sensors MODerate resolution Imaging Spectroradiometer (MODIS)  
17 onboard the Terra and Aqua satellites have been widely used in a variety of studies (Ahl et al. 2006; Busetto et al.  
18 2010; Colombo et al. 2011; Colombo et al. 2009; Hmimina et al. 2013; Eklundh et al. 2009; Sesnie et al. 2012;  
19 Song et al. 2013; Soudani et al. 2008; Zhang et al. 2003). Thanks to the two twin MODIS instruments, MODIS  
20 data are acquired globally twice per day per instrument at the spatial resolutions of 250 m, 500 m and 1 km at  
21 nadir, depending on the spectral band. MODIS imagery is distributed at various pre-processing levels and, with  
22 respect to the temporal resolution, data are released as both daily and composites products, the latter generated at  
23 different compositing steps (8-day, 16-day, monthly). Composite data have some advantages respective to daily  
24 data because the compositing process strongly reduces the effect of clouds, snow and noise (Holben 1986; Solano  
25 et al. 2010; Wolfe et al. 1998). On the other hand, the compositing process introduces temporal and spatial  
26 discontinuities since values from adjacent pixels may have been acquired on different dates, according to quality  
27 criteria. Moreover, the temporal resolution is degraded and may not be sufficient to accurate monitoring of rapid

1 transitions in vegetation dynamics (Ahl et al 2006; Holben 1986; Solano et al. 2010), especially in cases of  
2 compositing periods longer than 16 days (Zhang et al. 2009).

3 Various algorithms have been developed to model the behavior through time of physiological variables that can be  
4 tracked by satellite data, such as LAI (Leaf Area Index), FPAR (Fraction of Photosynthetically Active Radiation)  
5 or chlorophyll content (Rodriguez-Galiano et al. 2015). According to the available literature, in deciduous forests  
6 characterized by large seasonal changes in canopy leaf area, methods based on least-square fitting of logistic  
7 functions of time applied on time-series of satellite-derived vegetation indices led to estimations close to ground  
8 observations (Hird and McDermid 2009; White et al. 2009; Atkinson et al. 2012; Hird and McDermid 2009).

9 Those methods use analogy with phenology and growing degree-day models based on the assumption that  
10 vegetation phenology and growing are responsive to cumulative daily temperature, which can be represented by a  
11 logistic function of time (de Beurs and Henebry 2010a; Ratkowsky 1983; Richardson et al. 2006; Villegas et al.  
12 2001; Zhang et al. 2003). A number of different logistic functions have been used to derive the phenology  
13 information (Beck et al. 2006; Fisher et al. 2006; Hmimina et al. 2013; Soudani et al. 2008; Zhang et al. 2003)  
14 with the main differences between them being the phenological metrics considered, metrics algorithm extraction  
15 and the number of fitting parameters (four to eight). The logistic function proposed by Hmimina et al. (2013) is  
16 the one we implemented in this work since it is the latest improvement of the function proposed in Soudani et al.  
17 (2008) that in turn was based on the equation proposed by Zhang et al. (2003), the latter being that used in  
18 MODIS global vegetation phenology product (MCD12Q2). Several methods have been developed to extract Start  
19 of Season (SOS) and End of Season (EOS) dates from fitted vegetation index time-series (VI TS) generated from  
20 satellite data. TIMESAT (Jönsson and Eklundh 2002, 2004; Jönsson and Eklundh 2002; Jönsson and Eklundh  
21 2003; Jönsson and Eklundh 2004) extracts SOS and EOS according to fixed, user-defined thresholds as increase  
22 from spring minimum and decrease from summer maximum (Jönsson and Eklundh 2002, 2004). Zhang et al.  
23 (2003) and Ahl et al. (2006) used local minima and maxima of fitting functions' curvature to find onset and  
24 fullness of flushing and yellowing. Left and right inflection points derived from logistic functions were commonly  
25 used to represent SOS and EOS respectively (Beck et al. 2006; Fisher et al. 2006; Hmimina et al. 2013; Liang et  
26 al. 2011; Soudani et al. 2008). Since inflection points are in the middle of the function's amplitude (Fisher et al.  
27 2006; Soudani et al. 2008), they are equivalent to the TIMESAT fitting based on the logistic function algorithm  
28 with both SOS and EOS thresholds set to 0.50. Fixed VI thresholds were tested and compared to other extraction

1 methods, sometimes with results more related to ground phenology respective to the others (Studer et al. 2007),  
2 but a universally applicable VI threshold has not yet been recognized. A review is available in de Beurs and  
3 Henebry 2010b. In addition to the fact that there is no clear consensus on the most efficient extraction algorithms,  
4 there are no conclusions that emerge clearly from previous studies regarding the best performing VIs and the  
5 uncertainty of satellite-based estimates of phenological dates related to temporal resolution used in time-series  
6 composite data.

7 The aim of this work was to find the best combination of MODIS imagery and VI to estimate SOS and EOS. We  
8 used 2001 - 2012 daily reflectance and 16-day composite Normalized Difference Vegetation Index (NDVI) and  
9 Enhanced Vegetation Index (EVI) to generate TS of six vegetation indices (EVI, NDVI and four Wide Dynamic  
10 Range Vegetation Index (WDRVI)). From each VI/TS combination we extracted SOS and EOS and then  
11 compared them with eight ground phenological metrics measured in 50 plots composed by the main deciduous  
12 broad-leaf tree species belonging to the French RENECOFOR network (*Réseau National de suivi à long terme  
13 des ECOSystèmes FORestiers*). Authors acknowledge that the experimental design is not perfectly responding to  
14 a rigorous scientific approach: in particular available ground measures were not proper, both in terms of spatial  
15 representativeness and time sampling design for the goals of this work. Nevertheless it is authors' opinion that  
16 the further exploitation of already existing datasets, that someone got in the past for other goals different from the  
17 ones intended for this scientific work, is desirable for the following reasons: scientific knowledge can be however  
18 improved by optimizing economic resources (no additional costs have to be charged onto the project); science is  
19 moved towards a more operational context where the bottom (applications) requires that the top (science) certifies  
20 already existing conditions or data. The idea of a such challenging experience was suggested by the current  
21 diffused instances, also in forestry and agriculture (Lauer et al., 2014, Hirafuji, 2014), concerning data crowd  
22 sourcing and Big Data management and filtering. In fact, the problem is similar: existing data generated with no  
23 specific design, nor guaranteed, are exploited in a second time to extract the most of information under new  
24 controlled conditions able to certify their reliability, uncertainty and range of validity for that context.

25

## 26 **2 – Data**

27

### 28 **2.1 - Study area**

29 The study area was composed of 50 broadleaf forest plots, distributed across France (Figure 1).

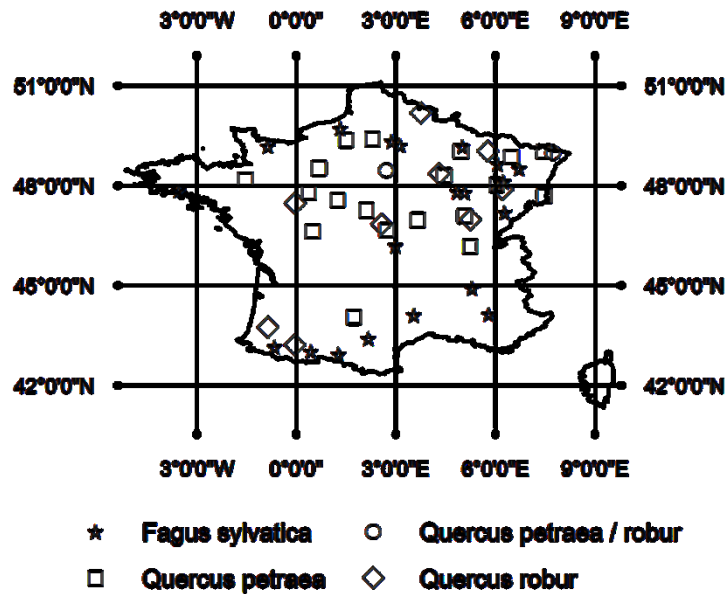


Figure 1 – Locations within France of the 50 study plots.

All of the 50 forest plots are covered by deciduous forest and are part of the RENECOFOR network, created in 1992 by the French National Forest Service aimed at long-term monitoring of forest ecosystems. It is the French part of a wider network that includes 34 European countries. The main tree species populating the 50 plots we considered are *Quercus robur* L. (pedunculate oak, 9 plots); *Quercus petraea* (Matt.) Liebl. (sessile oak, 19 plots); and *Fagus sylvatica* L. (beech, 20 plots). In two plots, pedunculate and sessile oaks are mixed. Ages range from 60 to 120 years; all plots have little or no slope.

Climate across the plots is generally temperate, with four climatic types: a) Mediterranean, on the south coast; b) Oceanic, along the west coast; c) Continental, in the inner part of the country; and, d) Alpine, at the highest elevations (Soudani et al. 2008). Elevation of the plots range from 20 to 320 m a.s.l. (200 m on average) for oak plots and 50 to 1,400 m for beech plots (560 m on average). Each plot extends over 2 ha and is covered by same-species and mature trees; 36 trees in the center of each plot are numbered, fenced and, in spring and autumn, monitored weekly. Each weekly observation is reported on the Monday of the week it refers to. Phenology of understory is monitored in the same way.

The reason we considered only deciduous vegetation is that the small yearly increase/decrease of VI values typical of evergreen canopies make logistic functions unsuitable for phenological investigations. Other methods should be used, e.g. splines (Hmimina et al. 2013).

1 **2.2 - In situ phenological observations**

2  
3 In this work, we compared phenological metrics (i.e. SOS, EOS) estimated from MODIS imagery with 8 types of  
4 phenological ground observations from the available stations of the RENECOFOR network (Table 1).

5 Table 1 - Phenological stages recorded within the RENECOFOR dataset.

	<b>Phenological Feature</b>	<b>Abbreviation</b>
SOS	Main species flushing 10%	MSp F 10%
	Understory flushing 10%	Und F 10%
	Main species flushing 90%	MSp F 90%
	Understory flushing 90%	Und F 90%
EOS	Main species yellowing 10%	MSp Y 10%
	Understory yellowing 10%	Und Y 10%
	Main species yellowing 90%	MSp Y 90%
	Understory yellowing 90%	Und Y 90%

6  
7 The 10% and 90% thresholds indicate the dates when 10% and 90% of each plot's trees have buds open (flushing  
8 phases) or yellow leaves (yellowing phases) over at least 20% of the crown (Bourjot et al. 2006). There is no  
9 official cross-walk of the RENECOFOR phenological stages to the BBCH-based phenological scale.  
10 RENECOFOR data refers to a weekly sampling design. Consequently, internal time uncertainty of ground data  
11 can be assumed varying between 4 and 12 days (one week) depending on the day when observations of two  
12 consequent weeks occurred.

13 **2.3 - Satellite data**

14  
15 This work was based on 12 years (2001-2012) of both daily and composite MODIS VIs (collection 5). All the  
16 imagery was acquired from the Land Processes Distributed Active Archive Center (LP DAAC) through the  
17 Reverb-Echo portal. The 50 MODIS 250 m pixels encompassing the center of each plot were the only ones  
18 extracted from the MODIS datasets.

19 **2.3.1 - MODIS products used in the study**

20  
21 2.3.1.1 - MOD09 GQ and MOD09GA daily surface reflectance

22 Daily red and near infrared (NIR) surface reflectances were acquired from the MOD09GQ (Terra) product  
23 (Surface Reflectance Daily L2G Global 250 m) at the geometric resolution of 250 m. Surface reflectances in the  
24 blue band (MODIS band 3), necessary to calculate EVI, were extracted at the 500 m resolution from the



1 MOD09GA (Surface Reflectance Daily L2G Global 1km and 500m) product. In cases where multiple  
2 observations were available on the same day, we selected the first layer (LP DAAC 2014).

3 Daily quality assessment (QA) flags, provided at 1 km resolution, were extracted from the MOD09GA product in  
4 order to gather information about the state of the atmosphere at the moment and in the position of the acquisition  
5 (presence of clouds, cirrus, aerosol concentration).

#### 6 2.3.1.2 - MOD13Q1 16-day composite vegetation indices

7 Composite VIs were acquired from the MOD13Q1 product (Vegetation Indices 16-Day L3 Global 250 m). It  
8 provides one NDVI and EVI value every 16 days, allowing the composition of gap-free TS. The per-pixel  
9 compositing algorithm is described in the MOD13Q1 product user guide (Solano et al. 2010).

10 The MOD13Q1 product includes, among the other layers: a) 16-day composite EVI and NDVI; b) QA  
11 information from the layer *250m 16 days pixel reliability summary QA* (PR); and, c) acquisition dates in the *250m*  
12 *16 days composite day of the year* layer (CDOY). The PR layer reports pixels' overall quality, while the CDOY  
13 layer contains the date each VI value was acquired. Beginning with collection 5, this layer was made available and  
14 dates are the same for both EVI and NDVI.

15 Within the MODIS mission, according to file names, the nominal date associated with each composite is its first  
16 day. Nevertheless, the actual acquisition date of each pixel (CDOY) usually differs from the nominal date since  
17 the acquisition may have occurred on any one of the 16 days embraced by every composite and the difference  
18 between the nominal date and the true date ranges 0 to 15 days. Previous research has shown that the adoption of  
19 the nominal date of composites can introduce temporal errors that potentially make a TS inadequate to correctly  
20 describe phenological patterns (Testa et al. 2014; Thayn and Price 2008).

#### 21 **2.4 - Vegetation indices**

22 VIs are commonly used for extracting phenological parameters. In the present study we considered EVI, NDVI  
23 and WDRVI at four levels.

25 NDVI (Tucker 1979) is the most known and used VI. Its strength is its rationing formulation, which allows the  
26 reduction of topographic effects, illumination conditions, cloud shadow and atmospheric attenuation (Huete et al.  
27 2002). It is mainly responsive to canopy chlorophyll content. Among the limitations, NDVI is known to lose  
28 sensitivity when a canopy's Leaf Area Index is greater than 3-5 (e.g., Davi et al. 2006; Soudani et al. 2006) due to

1 the extinction of radiation in both downward and upward directions and a reduced contribution from lower canopy  
 2 layers. Within the MODIS mission, NDVI is considered the “continuity index” for the more than 20-year-long  
 3 NOAA Advanced Very High Resolution Radiometer (AVHRR) mission (Huete et al. 2002). It is calculated  
 4 combining NIR and red reflectances as:

$$NDVI = \frac{NIR - red}{NIR + red} \quad (1)$$

5 where *red* and *NIR* are MODIS band 1 and 2 surface reflectances, respectively.

6 EVI is the vegetation index optimized for MODIS bands (Huete et al. 1999). It has been used in phenological  
 7 works, e.g. (Ahl et al. 2006; Sesnie et al. 2012; Setiawan et al. 2014), and in the MCD12Q2 MODIS product  
 8 (Land Cover Dynamics Yearly L3 Global 500 m). EVI is less widely used than NDVI because it needs, in  
 9 addition to red and near infrared bands, the blue one, not available for AVHRR data; the use of this vegetation  
 10 index at global scale is therefore limited to MODIS data (Jiang et al. 2008).

11 EVI is formulated as:

$$EVI = G \cdot \frac{NIR - red}{NIR + C_1 \cdot red - C_2 \cdot blue + L} \quad (2)$$

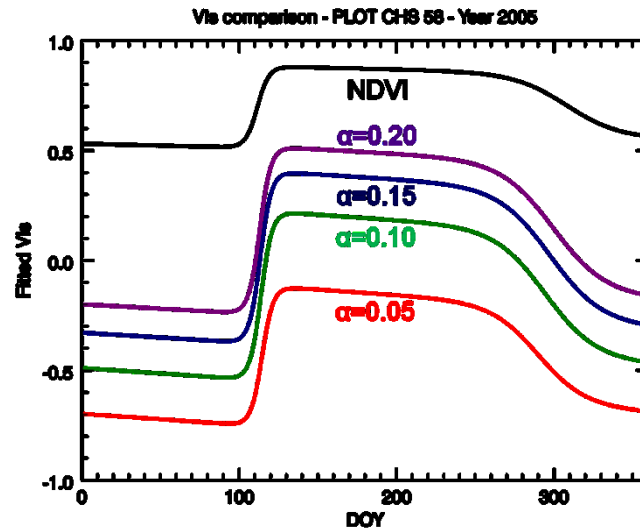
12 where *blue* is the reflectance in the blue band (MODIS band 3). “*L* is the canopy background adjustment that  
 13 addresses non-linear, differential NIR and red radiant transfer through a canopy, and  $C_1$ ,  $C_2$  are the coefficients of  
 14 the aerosol resistance term, which uses the blue band to correct for aerosol influences in the red band” (Huete et  
 15 al. 2002). The coefficients adopted to implement the MODIS EVI algorithm are:  $L = 1$ ,  $C_1 = 6$ ,  $C_2 = 7.5$ , and  $G =$   
 16  $2.5$  (gain factor). EVI seems to be less sensitive to saturation problems over dense canopies (Hufkens et al. 2012)  
 17 and reduces the influence of the background’s color and atmosphere (Xiao et al. 2003).

18 In order to linearize the relationship between LAI and NDVI, Gitelson (2004) proposed the WDRVI. It is  
 19 calculated as:

$$WDRVI = \frac{\alpha \cdot NIR - red}{\alpha \cdot NIR + red} \quad (3)$$

20 where  $\alpha$  -that is lower than 1.0- is the coefficient that reduces the contribution of NIR to the VI’s value.  $\alpha$  is added  
 21 to increase the contrast between red and near infrared reflected radiation by living vegetation and allows  
 22 significant enhancement of the linearity and the sensitivity of WDRVI, by comparison with NDVI, especially

1 under high biomass conditions (Gitelson, 2004). Figure 2 shows variations in annual amplitude of WDRVI  
 2 depending on  $\alpha$ .



3  
 4 Figure 2 – Fitted TS of NDVI (black) and WDRVI as a function of the  $\alpha$  parameter (red, green, blue, purple) of the plot CHS 58, year  
 5 2005.  
 6

7 By rearranging the terms of equation (3), WDRVI can be calculated as a function of NDVI (Viña and Gitelson  
 8 2005):

$$WDRVI = \frac{(\alpha + 1) \cdot NDVI + (\alpha - 1)}{(\alpha - 1) \cdot NDVI + (\alpha + 1)} \quad (4)$$

9 with  $\alpha = [0.05, 0.10, 0.15, 0.20]$ . WDRVI was originally introduced for agricultural monitoring, and it has not yet  
 10 been extensively tested for forest phenology monitoring (Eklundh et al. 2009).

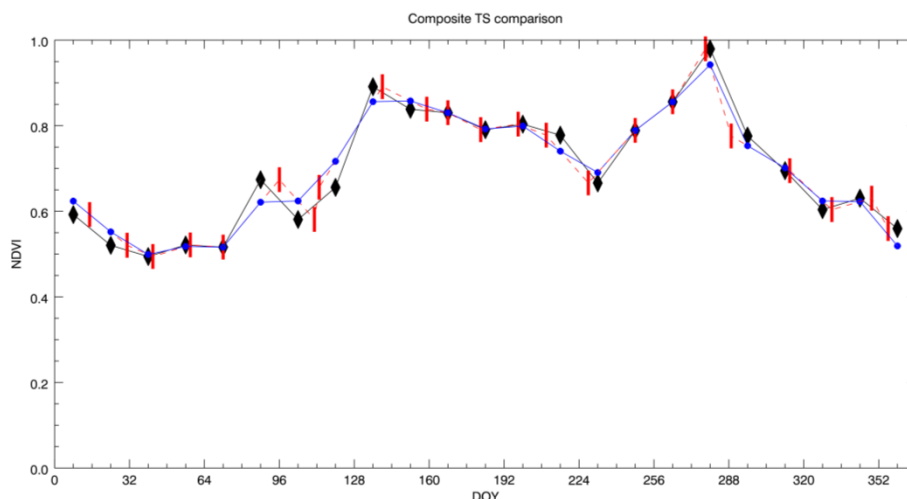
### 11 3 – Data analysis

12  
 13 The following are the main processing steps we carried out: a) TS generation; b) reduction of noise in TS by  
 14 removal of low quality observations (i.e. contaminated by clouds, shadows, aerosol) and filtering; c) estimation of  
 15 SOS and EOS; and, d) quality analysis of SOS and EOS estimates by comparison with ground measurements of  
 16 RENECOFOR plots.

#### 17 3.1 - Time series generation

18 Daily reflectances from the MOD09GQ/A products were used to compute daily 250 m EVI and NDVI TS.  
 19 Calculation of daily EVI required 500 m blue band, combined with the 250 m red and NIR bands. WDRVI time  
 20 series were generated from NDVI, as described in equation (4). Four WDRVI implementations were tested in this  
 21 work, each one corresponding to a different value of the  $\alpha$  coefficient:  $WDRVI_{0.05}$ ,  $WDRVI_{0.10}$ ,  $WDRVI_{0.15}$ , and  
 10

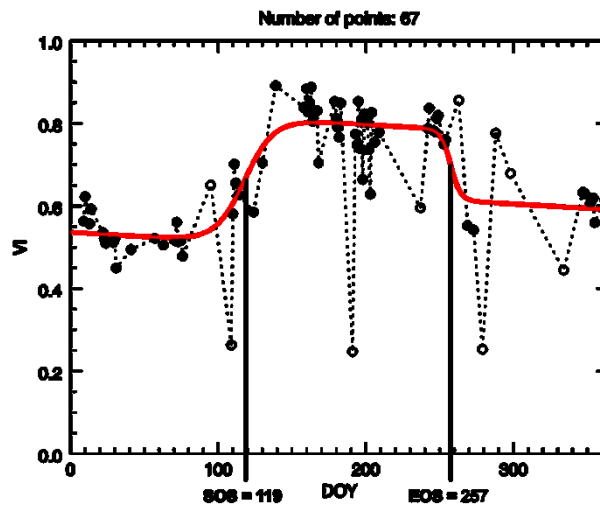
1 WDRVI<sub>0.20</sub> where the value of  $\alpha$  was expressed by the subscripts. Each VI TS came with a corresponding QA TS,  
 2 extracted from the MOD09GA dataset. 16-day composite EVI and NDVI TS were directly extracted from the  
 3 correspondent MOD13Q1 layers, and the WDRVI was derived from the NDVI TS (eq. 4).  
 4 Four TS were generated from MOD13Q1 datasets (Figure 3):  
 5 A) Raw TS (hereafter MOD13<sub>RAW</sub>), i.e. VIs as supplied by the MOD13 product. VI values were formally  
 6 equidistant in time, but this was not accurate, since VI values could have been acquired at any point within the 16-  
 7 day compositing period, making potential time distances between two consequent observations ranging from 1 to  
 8 31 [16 days/compositing period x 2 compositing periods – 1] days. Based on previous works (Testa et al. 2014),  
 9 we considered MOD13<sub>RAW</sub> values nominally placed in the centre of each compositing period (the 8<sup>th</sup> day).  
 10 B) Raw TS adjusted with regards to acquisition dates (MOD13<sub>AD</sub>). Index values were the same as MOD13<sub>RAW</sub>,  
 11 but acquisition dates were adjusted before fitting. This resulted in a new TS not equally spaced in time.  
 12 C) One of the assumptions of some algorithms (e.g. the Fast Fourier Transform) and software (e.g. TIMESAT) is  
 13 that TS data are equidistant. According to the procedure described in Testa et al. (2014), we resampled the  
 14 MOD13<sub>AD</sub> TS to the nominal dates (the 8<sup>th</sup> day in this work, as noted above), making it equidistant in time but  
 15 with VI values linearly adjusted. TS treated according to this procedure are hereafter called MOD13<sub>ALIGNED</sub>.  
 16 D) The fourth way we managed composite data was aimed at creating a hybrid, pseudo-daily TS (MOD13<sub>Daily</sub>):  
 17 we performed a daily linear interpolation of the MOD13<sub>AD</sub> TS. The underlying idea was to create daily, gap-free  
 18 TS from the less noisy composite, date-corrected MOD13<sub>AD</sub> TS.



19  
 20 Figure 3 - NDVI TS generated from the MOD13Q1 product inherent the plot CHP10 (48°20'51" N, 4°18'17" E, elevation: 115 m  
 21 a.s.l.), year 2006. Plot's main species was pedunculate oak; the understory species was hornbeam. Diamonds, solid line: MOD13<sub>RAW</sub>  
 22 (A); vertical bar, dashed line: MOD13<sub>AD</sub> (B); empty circle, dotted line: MOD13<sub>ALIGNED</sub> (C). MOD13<sub>DAILY</sub> (D) is not expressly  
 23 reported since it overlays MOD13<sub>AD</sub> TS.  
 24

25 **3.2 - TS preprocessing**  
 11

1 Time series were preprocessed by removing observations contaminated by clouds, shadows and snow. Only pixels  
 2 whose QA flags reported no contamination were considered.  
 3 Then, a moving median filter was run on daily TS to reduce noise (Hmimina et al. 2013; Soudani et al. 2008).  
 4 Given a 5-day moving window, its median was calculated at each step and VI values outside the  $median \pm 20\%$   
 5 range were discarded, as proposed by Soudani et al. (2008). Figure 4 indicates the effect of the median filter on  
 6 daily NDVIs for the oak plot CHP10, year 2006.  
 7



8  
 9 Figure 4 - NDVI for the plot CHP10, year 2006. Solid Circles: Daily NDVI values; Open circles: observations rejected by the median  
 10 filter. Red line: fitted ndVI. Left vertical line: left inflection point (SOS), right vertical line: right inflection point (EOS). In this case,  
 11 SOS and EOS dates were estimated to be on DOY 119 and 257, i.e. April, 25<sup>th</sup> and September 14<sup>th</sup>, respectively.  
 12

### 13 3.3 - Time Series Fitting and Estimation of SOS and EOS

14 We modelled VI TS performing iterative Least Square fitting of the asymmetric double logistic function proposed  
 15 by (Hmimina et al. 2013):  
 16

$$VI_t = p \cdot t + (a + c) + \frac{1}{2}(a - c) \cdot \tanh[b \cdot (t - SOS)] - \frac{1}{2}(a - e) \cdot \tanh[d \cdot (t - EOS)] \quad (5)$$

17 where  $VI_t$  is the fitted VI value at time  $t$ , SOS and EOS are the start of season and end of season date, and  $a, b, c,$   
 18  $d, e, p,$  are the parameters of the curve.  $p$  accounts for the slight linear decrease in VI TS during winter and  
 19 summer, observed in VI TS over deciduous broadleaf forests as underlined in previous studies (Soudani et al.  
 20 2012; Elmore et al. 2012; Hmimina et al. 2013; Melaas et al. 2013).

1 The parameters of equation (5), including SOS and EOS, were estimated separately for each plot and for each  
 2 year.

3 We tested all the possible solutions obtained by changing (with a time increment of 3 days) the initializations of  
 4 the model's parameters SOS and EOS within a reasonable time period (search window), deduced from the average  
 5 phenology of broadleaf forests in temperate regions of the Northern Hemisphere (Table 4). It resulted in a total of  
 6 2025 (45<sup>2</sup>) combinations of SOS and EOS for each pixel/year.

7

8 Table 4- Minimum and maximum values of the search windows.  
 9

	<b>MIN [DOY]</b>	<b>MAX [DOY]</b>	<b>Range [days]</b>
<b>SOS</b>	50 (19 <sup>th</sup> Feb.)	185 (4 <sup>th</sup> July)	135
<b>EOS</b>	210 (29 <sup>th</sup> July)	355 (21 <sup>st</sup> December)	135

10

11 For every combination of initialized SOS and EOS, a least square fitting was run. The minimum Root Mean  
 12 Square Error (RMSE) between the given raw TS and each of the 2025 fitted TS, calculated for each of the 2025  
 13 solutions as in equation (6), was the driver to select the best fit.

$$RMSE_{FIT} = \sqrt{\frac{\sum_{n=1}^n (VI_{raw} - VI_{fit})^2}{n - 1}} \quad (6)$$

14 SOS and EOS values corresponding to the selected solution were assigned to the site for the given year.

15 SOS or EOS estimation that fell out of the respective search windows were considered outlying estimations, and  
 16 thus were excluded from the computation of the results. No considerations were made for climatically anomalous  
 17 years.

### 18 **3.4 - Performance metrics**

19  
 20 2001-2012 SOS and EOS estimations were generated with the procedure described above for each of the 6 VIs  
 21 (EVI, NDVI, WDRVI<sub>0.05</sub>, WDRVI<sub>0.10</sub>, WDRVI<sub>0.15</sub>, WDRVI<sub>0.20</sub>), and for each of the considered TS (daily,  
 22 MOD13<sub>RAW</sub>, MOD13<sub>AD</sub>, MOD13<sub>ALIGNED</sub>, MOD13<sub>DAILY</sub>), resulting in 30 SOS and EOS values for each pixel/year.  
 23 Each pixel/year SOS/EOS estimation was compared with the four corresponding values (SOS and EOS for main  
 24 tree species and understory) recorded within the RENECOFOR dataset (Table 1).

1 Results were summarized in terms of mean error ( $\mu$ ) and root mean square deviation (RMSD).  $\mu$  is a measure of  
 2 bias of satellite estimations respective to ground phenology, while RMSD is a measure of the real uncertainty of  
 3 estimation. Metrics were aggregated and averaged on a per-year basis, i.e., for both SOS and EOS. All of the  
 4 values (up to fifty) from every year were averaged, resulting in eight 12-year (i.e. 12 values) long TS. We  
 5 assumed as best estimator (i.e. the best combination of VI and satellite data) the one that achieved the lowest  $\mu$   
 6 and RMSD values, ideally  $\mu = 0$  and  $RMSD \leq 7$ .

7 In particular, for each comparison and ground parameters,  $\mu$  was calculated as:

$$\mu = \frac{\sum_{y=1}^{12} \left( \frac{\sum_{i=1}^{50} (P_{ei,y} - P_{oi,y})}{50} \right)}{12} \quad (7)$$

8 where  $P_{ei}$  is the value of the phenological metric (SOS or EOS) estimated from satellite data, and  $P_{oi}$  is the same  
 9 variable observed on the ground for plot  $i$  in year  $y$ . Negative bias ( $\mu < 0$ ) means that MODIS-derived estimation  
 10 was anticipated with respect to ground data. On the contrary, positive bias ( $\mu > 0$ ) means that estimates were  
 11 delayed. RMSD were calculated according to equation 8:

$$RMSD = \frac{\sum_{y=1}^{12} \left( \sqrt{\frac{\sum_{i=1}^{50} (P_{ei,y} - P_{oi,y})^2}{50 - 1}} \right)}{12} \quad (8)$$

12 It is important to consider that ground observations were carried out weekly and that each observation referred to  
 13 the Monday of the week to which it belonged. Consequently, if  $RMSD \leq 7$  days, it can be said that VI TS based  
 14 estimation was as precise as field surveys.

## 15 **4 – Results**

### 16 **4.1 – Analysis of ground-based phenological observations**

17 In order to allow a better understanding of the estimated SOS and EOS from MODIS time-series, descriptive  
 18 statistics of ground-based phenological observations are shown (Figure 5).  
 20

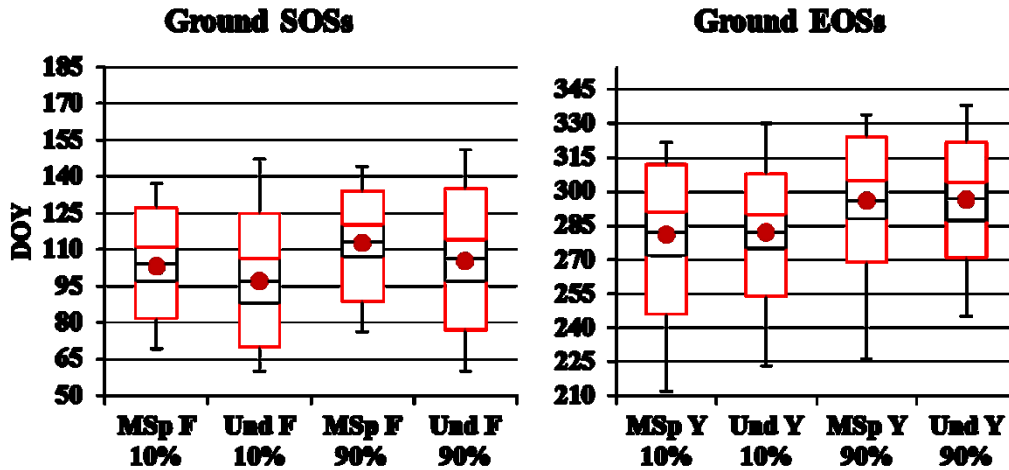


Figure 5 - Temporal distribution of the eight RENECOFOR phenological markers. Observations from all plots and all years were pooled. Left: Start of growing Season (SOSs); right: End of growing Season (EOSs). Black boxes: 1<sup>st</sup> to 3<sup>rd</sup> quartile, that is 50% of the values. Red boxes: 2.5<sup>th</sup> to 97.5<sup>th</sup> percentile, that embrace 95% of the observations. Black whiskers: minimum and maximum value of each distribution; red dots: average value.

In general, SOS dates were less variable than EOS dates; moreover, SOS dates of main species were less dispersing than the understory's' SOS dates. Considering ground plots pooled all together for both SOS and EOS, it was clear that the average distance in time between variables was much less than their internal dispersion, making single phenological stages hard to separate from each other because of the overlaps (Figure 5).

An overview of median time distances between ground phenological stages is shown in Table 5. Relative median temporal distances between ground parameters were calculated as relative difference respective to MSp 90% dates separately for both SOS and EOS.

Table 5 shows that, during spring, understory started generally earlier than main species trees. In fact, when understory reached the 90% level, main species just reached their 10% level.

The pattern shown by EOSs was much different: both understory's and main species' 10% events appeared on the same DOY on median, and a difference of only 1 day was found between main species and understory 90% yellowing stages. It is worth to remind that reported statistics, and in particular relative differences, concern inter-plot variability, with no regards about single observation uncertainty (ranging from 4 to 12 days, see Data paragraph) that it is expected to heavily condition accuracy of estimates from satellite.

Table 5- Timing of phenophases and distance in time relative to main species 90% flushing and yellowing. MSp 90% parameters were the reference. Highlighted in grey is the reference parameter.

SOSs			EOSs		
Phenophase	Median [DOY]	Relative difference [days]	Phenophase	Median [DOY]	Relative difference [days]



<b>MSp F 10%</b>	104	-9	<b>MSp Y 10%</b>	282	-14
<b>Und F 10%</b>	97	-16	<b>Und Y 10%</b>	282	-14
<b>MSp F 90%</b>	113	0	<b>MSp Y 90%</b>	296	0
<b>Und F 90%</b>	106	-7	<b>Und Y 90%</b>	297	1

1

## 2 4.2 - Satellite estimates

3

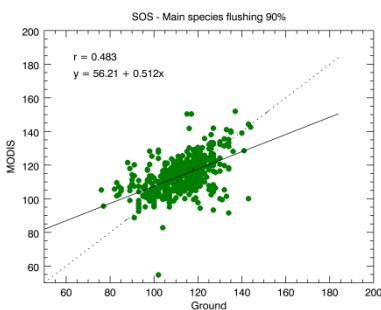
4 Main results from all comparisons between estimated and observed SOS and EOS are summarized in Figures 6, 7  
5 and 8. In order to simplify the evaluation of the results reported in Table 6, we extracted the best VI/TS  
6 combinations for both SOS and EOS, separately. We considered “best SOS combinations” those SOS VI/TS  
7 combinations that achieved simultaneously  $\mu = 0 \pm 3$  days and  $\text{RMSD} \leq 14$  days. The first measure corresponds to  
8 unbiased estimations  $\pm$  the length (in days) of 1 increment of procedure selecting the optimal fit; the latter  
9 corresponds to  $\text{RMSD} \leq$  two times the accuracy of the RENECOFOR dataset. At the same time, since EOS  
10 estimations were poorer in quality than SOS, we doubled the ranges of acceptable  $\mu$  and RMSD, considering “best  
11 EOS estimations” those that achieved simultaneously  $\mu = 0 \pm 6$  days and  $\text{RMSD} \leq 28$  days. Results are illustrated  
12 in Figure 6 for best SOS VI/TS combinations and in Figures 7 and 8 for best EOS VI/TS

### 13 4.2.1 – SOSs

14 Advanced greening of main species’ canopies (MSp F 90%) was the only SOS ground parameter that the  
15 combination of VI and TS we considered could estimate meeting the above-mentioned quality requirements ( $\mu = 0$   
16  $\pm 3$  days and  $\text{RMSD} \leq 14$  days). Performances achieved by such combinations are reported in Figure 6. VI/TS  
17 combinations are sorted according to a least-RMSD criterion (values are sorted first by increasing RMSD and then  
18 by increasing  $\mu$ ).

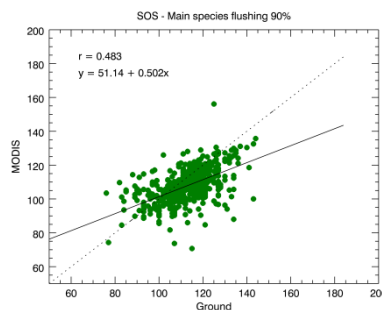
19

MOD13<sub>DAILY</sub>, EVI,  $\mu/\text{RMSD}$  1/10



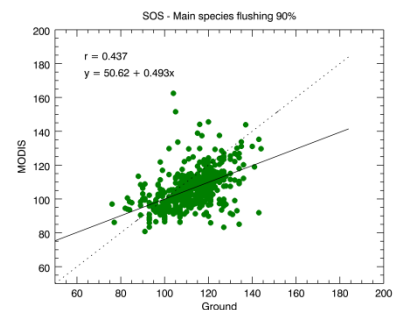
DAILY, EVI, 3/11

MOD13<sub>ALIGNED</sub>, WDRVI<sub>0.20</sub>, 3/10

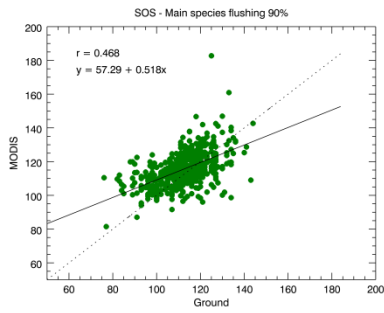


MOD13<sub>RAW</sub>, WDRVI<sub>0.15</sub>, 3/11

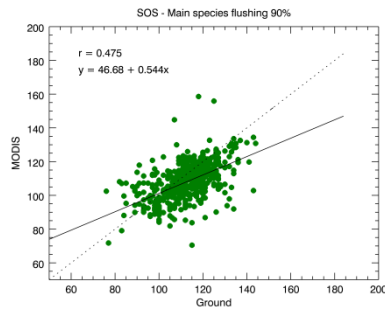
MOD13<sub>ALIGNED</sub>, EVI, 2/11



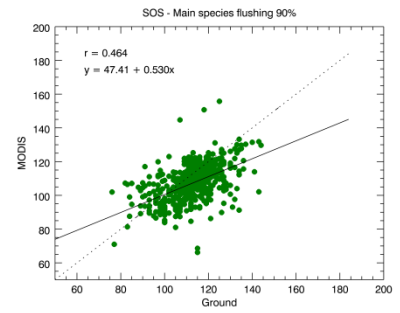
MOD13<sub>RAW</sub>, WDRVI<sub>0.20</sub>, 3/11



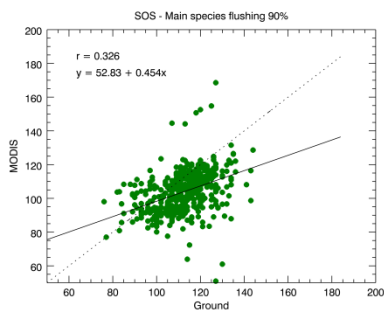
MOD13<sub>RAW</sub>, NDVI, 0/12



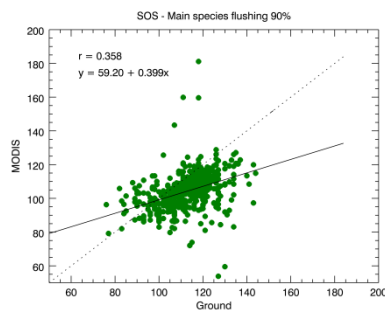
MOD13<sub>ALIGNED</sub>, NDVI, 0/12



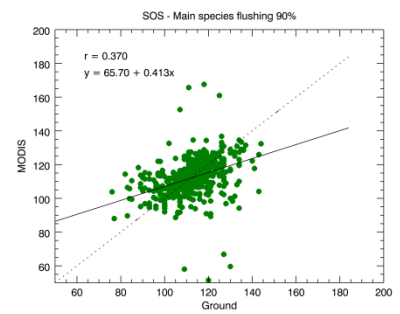
MOD13<sub>DAILY</sub>, NDVI, 0/12



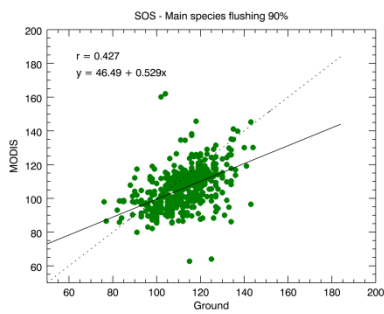
MOD13<sub>RAW</sub>, EVI, 2/12



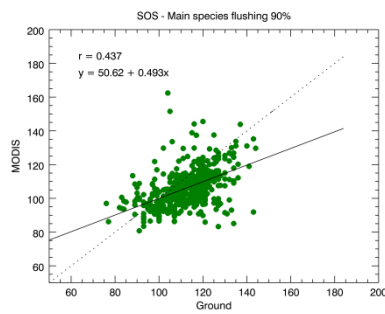
MOD13<sub>AD</sub>, EVI, 3/12



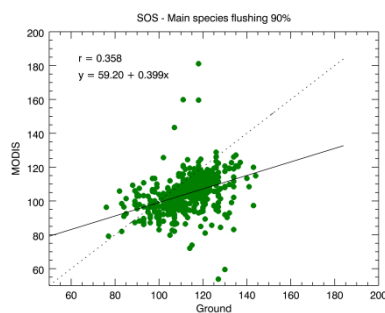
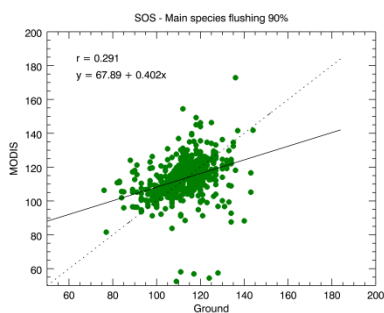
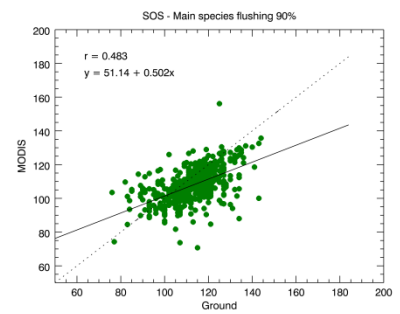
MOD13<sub>AD</sub>, WDRVI<sub>0.20</sub>, 3/12



DAILY, NDVI, 1/13



MOD13<sub>AD</sub>, NDVI, 0/14



1  
2  
3  
4  
Figure 6 - SOS best results: MODIS/ground scatter plots of the best SOS estimations. The label above each plot contains, in the following order: TS type, VI,  $\mu$ /RMSD (in days). In spite of scatterplots and low R values, all tested correlation showed to be significant at  $p < 0.05$ .

1 Among the best SOS results, all NDVI-based estimations were biased no more than 1 day in all comparisons with  
 2 RMSDs ranging between 12 to 14 days. EVI, WDRVI<sub>0.15</sub> and WDRVI<sub>0.20</sub> showed 1 to 3 day biases, but lower  
 3 RMSDs (10 to 12 days compared to 12 to 14).

4 Considering the RMSD-based rank we proposed in Figure 6, EVI implemented from MOD13<sub>DAILY</sub> TS was the  
 5 best-performing VI/TS combination, followed by WDRVI<sub>0.20</sub> implemented with MOD13<sub>ALIGNED</sub> TS. If a zero-bias  
 6 approach is preferred, NDVI implemented with MOD13<sub>RAW</sub>, MOD13<sub>ALIGNED</sub> and MOD13<sub>DAILY</sub> TS were the best-  
 7 ranked solutions.

#### 8 4.2.2 - EOSs

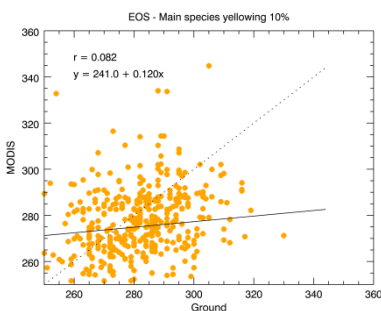
9  
 10 Within the best EOS combinations reported in Figures 7 and 8, considering only those referred to main trees  
 11 phenology, we found that: a) WDRVI<sub>0.05</sub> lead to the best estimations of initial yellowing (M<sub>Sp</sub> Y 10% parameter)  
 12 across most TS; b) EVI lead to the best estimations of advanced yellowing (M<sub>Sp</sub> Y 90%) across most  
 13 comparisons.

14 Looking at the scatter plots, it is clear that the procedure did not allow precise EOS estimations because of the  
 15 considerable errors at the single-estimation scale (sparse scatter plots).

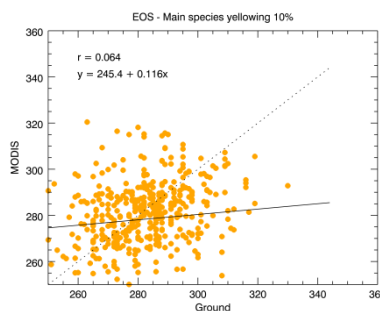
16 Figure 7 reports the best VI/TS combinations respective to early EOS comparisons. It shows that WDRVI<sub>0.05</sub>  
 17 achieved the lower biases (1 to 2 days) and, when implemented based on MOD13<sub>ALIGNED</sub> TS, allowed the best  
 18 performance (i.e. least RMSD AND least  $\mu$ ).

19

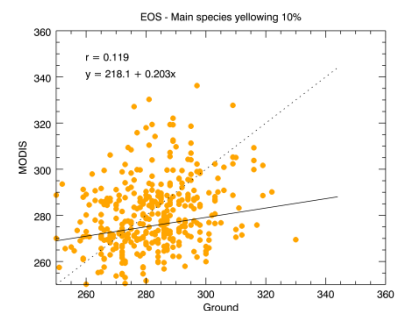
MOD13<sub>ALIGNED</sub>, WDRVI<sub>0.05</sub>, 2/23



MOD13<sub>ALIGNED</sub>, WDRVI<sub>0.10</sub>, 5/23



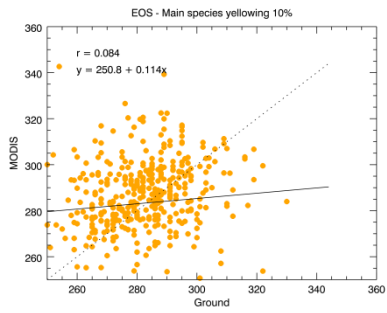
MOD13<sub>RAW</sub>, WDRVI<sub>0.05</sub>, 2/24



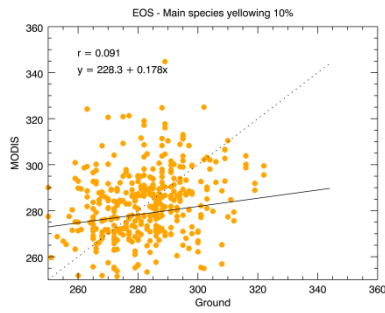
MOD13<sub>DAILY</sub>, WDRVI<sub>0.05</sub>, 2/25

MOD13<sub>RAW</sub>, WDRVI<sub>0.10</sub>, 5/25

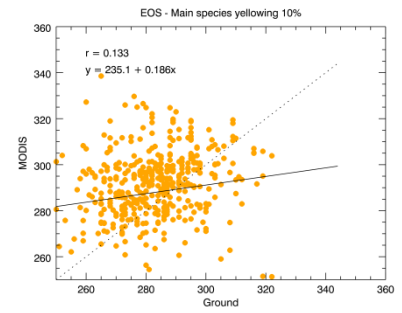
MOD13<sub>DAILY</sub>, WDRVI<sub>0.10</sub>, 6/25



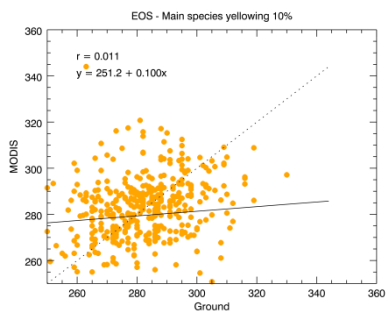
MOD13<sub>ALIGNED</sub>, WDRVI<sub>0.15</sub>, 6/25



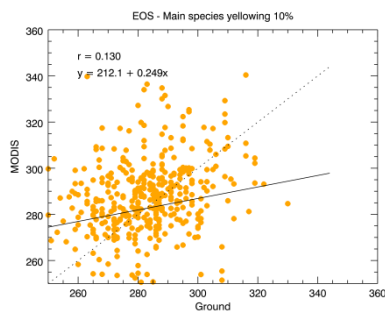
MOD13<sub>AD</sub>, WDRVI<sub>0.05</sub>, 1/26



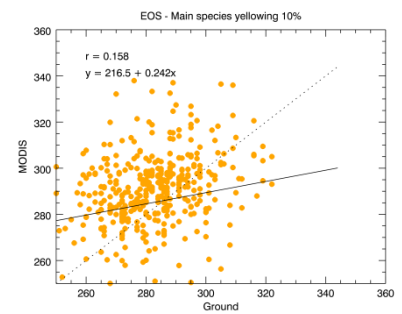
MOD13<sub>AD</sub>, WDRVI<sub>0.10</sub>, 4/26



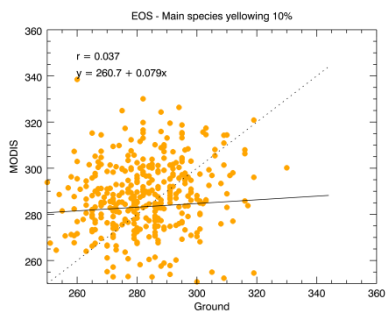
DAILY, WDRVI<sub>0.05</sub>, 2/27



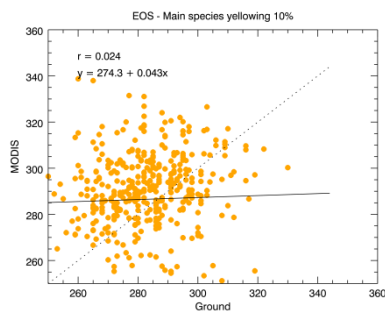
DAILY, WDRVI<sub>0.10</sub>, 6/27



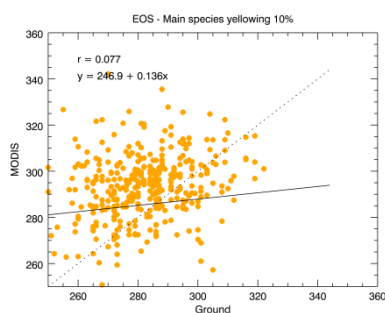
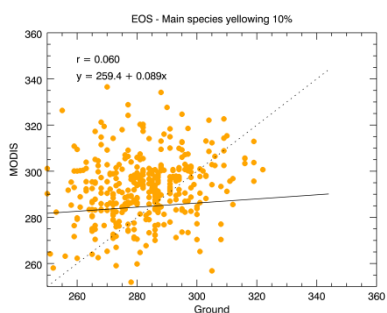
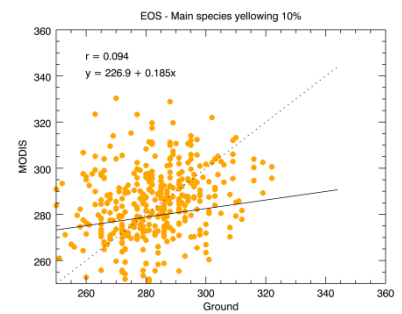
MOD13<sub>RAW</sub>, WDRVI<sub>0.15</sub>, 6/27



MOD13<sub>AD</sub>, WDRVI<sub>0.15</sub>, 4/28



MOD13<sub>AD</sub>, WDRVI<sub>0.20</sub>, 4/28

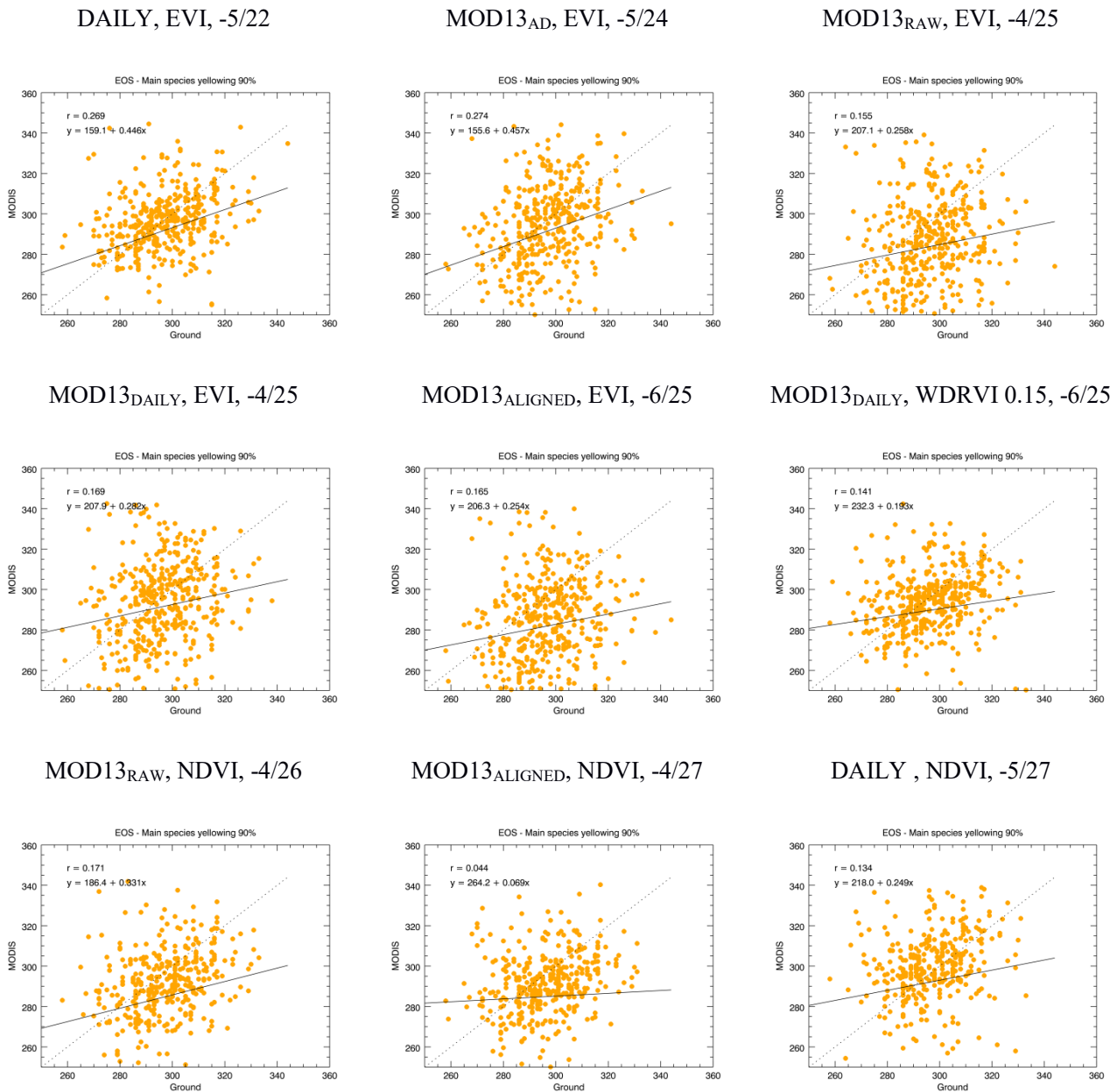


1 Figure 7 - Early EOS best results: MODIS/ground scatter plots of the best early EOS estimations. The label above each plot contains,  
 2 in the following order: TS type, VI,  $\mu$ /RMSD. In spite of scatterplots and low R values, all tested correlation showed to be significant  
 3 only at  $p < 0.15$  (therefore not reasonably acceptable for practical purposes).  
 4

1 Figure 8 shows the best VI/TS combinations regarding advanced EOS estimation (M<sub>Sp</sub> Y 90%). According to the  
 2 least-RMSD ranking, the best estimations were obtained by daily EVI, followed by EVI implemented on  
 3 MOD13<sub>AD</sub> TS. NDVI performed slightly worse in terms of RMSD.

4

5 Figure 8 - Advanced EOS best results: MODIS/ground scatter plots of the best advanced EOS estimations. The label above each plot  
 6 contains, in the following order: TS type, VI,  $\mu$ /RMSD (in days).  
 7



8

9 Figure 8 - Advanced EOS best results: MODIS/ground scatter plots of the best advanced EOS estimations. The label above each plot  
 10 contains, in the following order: TS type, VI,  $\mu$ /RMSD (in days). In spite of scatterplots and low R values, all tested correlation  
 11 showed to be significant only at  $p < 0.15$  (therefore not reasonably acceptable for practical purposes).  
 12

## 1 **5 – Discussions**

2

3 From a technical point of view, in addition to the effects of temporal resolution and the distribution of the values  
4 in the VI time-series, the ability of the asymmetric double logistic function to describe finely the seasonal pattern  
5 of phenology in deciduous broadleaf forests is strongly dependent on the initialization of parameters. This is even  
6 more problematic since the model proposed in Hmimina et al. (2013) (Eq.5) adds a supplementary parameter to  
7 account for the monotonic decrease of VI over the winter and summer seasons. In this work, we developed an  
8 automatic per-pixel procedure that performed least square fittings of equation (5). It is well known that not-linear  
9 In our procedure, a SOS and an EOS temporal search window were given, and day of year from such windows  
10 were used to sequentially extract initialization values of the parameters SOS and EOS, resulting in 2025 fitted TS.  
11 This new procedure allowed us to reduce significantly uncertainty in generating SOS and EOS phenological  
12 metrics from fitted VI TS.

13 SOSs and EOSs were estimated for each combination of VI and TS (6 VIs by 5 TS = 30 combinations) and such  
14 SOS/EOS estimations were compared against the corresponding set of 4 SOS and 4 EOS parameters from the  
15 RENECOFOR dataset. Average bias ( $\mu$ ) and RMSD were the statistics we computed to evaluate the performance  
16 of every VI/TS combination.

17 In terms of errors (RMSD) between observed and predicted phenological metrics, SOS estimations were more  
18 precise and accurate than EOSs (10 days vs 22 days for best VI/TS combinations). This result agrees with the  
19 conclusion outlined in the MODIS phenology assessment works in the studies of Ganguly et al. (2014) and Zhang  
20 et al. (2006), that MODIS-based estimates of the end of growing season have larger uncertainty than the start of  
21 season. As noted in Soudani et al. (2012) and in Hmimina et al. (2013), the spring flush and leaf development and  
22 expansion in deciduous broadleaf forests are, in absence of extreme cold and freeze events, relatively fast and  
23 lasts between 20 and 40 days in beech and oak forests in France (Soudani et al. 2008; Soudani et al. 2012). This  
24 period is also surrounded by two periods, the unleafy season in winter and the maximum LAI stage in summer.  
25 During these two periods, VI temporal variations are relatively small, and consequently, the fit is more  
26 constrained and the inflection point is likely well determined.

27 From a vegetation point of view, the analysis of the pattern of ground data found that, on average, bud burst of  
28 understory was earlier in spring by about 7 days respective to main species. When main species green up was  
29 beginning (10% F), understory was already reaching the 90% level. Since understory greening was generally

1 earlier than that of overlaying canopies, the first increase of surface greenness observed from MODIS was  
2 potentially related to the understory rather than to overstory trees (our target). Despite this, the least biased SOS  
3 estimations were found respective to the advanced greening of main trees (M<sub>Sp</sub> F 90%), meaning that MODIS  
4 estimations were more aligned to main trees greening rather than understory greening.

5 EOS estimations were affected by great uncertainty. This was possibly due to the greater complexity of autumnal  
6 leaf dynamics. Leaf yellowing, browning, marcescence and abscission, the mechanical influence of wind and  
7 precipitation, and the background effect of the soil covered by freshly-fallen leaves make the decrease in values of  
8 VIs generally slower and less uniform in autumn than the increase in spring (Hmimina et al. 2013; Nagler et al.  
9 2000; van Leeuwen and Huete 1996).

10 In terms of bias, it can also be noted that, considering M<sub>Sp</sub> F 90% vs M<sub>Sp</sub> Y 90%, SOSs are both less and  
11 inversely biased than EOSs (1 day versus -5 days for best combinations). The small bias obtained SOSs means  
12 that the inflection point of the fit is a robust marker of the foliage development and expansion during the spring  
13 and confirms the results obtained in Hmimina et al. 2013 which focused on comparing MODIS and ground-based  
14 NDVI TS. The bias in SOSs obtained using the other VI/TS combinations are also positive indicating that  
15 MODIS-based estimates occur later than in situ phenological observations. By contrast, EOSs are negatively  
16 biased at M<sub>Sp</sub> Y 90%, meaning that MODIS-based estimates anticipate the phase of onset of yellowing, but there  
17 are less and positively biased at M<sub>Sp</sub> Y 10%. According to the RENECOFOR dataset, understory and main  
18 species yellowed almost together on average, and consistent differences were only recorded between initial and  
19 advanced yellowing. Satellite EOS estimations were less biased respective to early yellowing, meaning that the  
20 right inflection point of equation (5) was closer to the initial loss of greening rather than to advanced yellowing.

21 With regard to SOS, main trees advanced flushing (M<sub>Sp</sub> F 90%) was the only phenological stage that could be  
22 estimated meeting the quality standard we set ( $\mu=0 \pm 3$  days,  $\text{RMSD} \leq 14$  days). Among the best SOS  
23 combinations (Figure 6), NDVI allowed the least biased estimations (less than 1 day in every combination), but it  
24 showed slightly higher RMSDs compared to EVI and WDRVI<sub>0.20</sub>. The best performance was obtained by  
25 EVI/MOD13<sub>DAILY</sub> TS, but the use of such a combination was very expensive in terms of computation time  
26 (365/366 values had to be fitted instead of less than 23 in the case of the other composite TS). Because of this, the  
27 use of both EVI or WDRVI<sub>0.20</sub> implemented from MOD13<sub>ALIGNED</sub> TS would be more suitable when computation  
28 time is a limiting factor.

1 In our study, the combination  $WDRVI_{0.05}/MOD13_{ALIGNED}$  was the choice that allowed the best estimation of early  
2 yellowing (Figure 7); daily EVI was instead the best estimator of advanced yellowing with performances very  
3 similar to those achieved by  $EVI/MOD13_{AD}$  TS (Figure 8). Advanced EOS estimations were generally less precise  
4 and accurate than early EOS estimations.

5 Finally, as underlined above, the phenomenon of senescence is a of great complexity and it is not surprising to  
6 note that compared to the spring leaf unfolding, there are less studies, both in vegetation phenology modeling and  
7 remote sensing, which were interested in the prediction of the date of senescence. Delpierre et al. (2009, 2015)  
8 emphasized the less attention given to the timing of leaf senescence, especially in modeling, and explained that  
9 this is probably due to the fact that the variability of the timing of leaf senescence seems to have less importance  
10 on the productivity of the ecosystems since the senescence occurs when conditions of temperature and radiation  
11 are less favorable to photosynthesis. The authors also highlighted the complexity of the senescence phenomenon,  
12 which is slower, more diffuse and involves numerous processes. The same observation about the lack of studies  
13 interesting in remote sensing of leaf senescence can be made as pointed out in Elmore et al. (2012).

14 While satellite-based estimates of SOS appear to be sufficiently accurate and can be used with some confidence,  
15 estimates of EOS should be considered with great caution because of their large uncertainties. The use of such  
16 estimates in climate-vegetation interactions may lead to misinterpretation. Further remote sensing studies of the  
17 timing of senescence are therefore necessary. However, these studies must be based on phenological observations  
18 using ground-based sampling that considers that remote sensing-based phenology is a pixel-scale phenology. The  
19 sampling design must consider the spatial resolution of the sensors, the spatial distribution of overstory and  
20 understory species and between and within species phenological variations. The sampling design used in the  
21 RENECOFOR network, originally constituted to monitor the health of forests, allows gathering phenological  
22 observations at the stand scale. However, observations are made in permanent plots of 2 ha each, i.e. about 1/3 of  
23 a MODIS 250 m pixel footprint. The sampling design is species-centered, not a pixel-centered, since observations  
24 are only made in homogeneous mono-specific plots and concern only overstory and understory trees, and does not  
25 provide any phenological information on the understory herbaceous and shrub vegetation. Moreover, time  
26 sampling design of RENECOFOR observations (once a week, and not always in the same day) makes reference  
27 dataset internally highly varying, determining a not controllable variability of differences between estimates and



1 observations and determining the impossibility of separating responsible error in final estimates. In spite of these  
2 limiting experimental conditions, we strongly believed that available datasets  
3 EVI, NDVI, WDRVI<sub>0.05</sub> and WDRVI<sub>0.20</sub> showed similar performances across different TS in estimating a given  
4 phenological parameter (Figure 6). In addition, daily MOD09 TS did not perform significantly better than  
5 MOD13 composite TS, if actual acquisition date is considered. In our opinion, this happened because the data  
6 (and, thus, the spectral content) underlying all TS was the same, i.e. daily reflectances. Combinations based on  
7 MOD13<sub>RAW</sub> TS should have led to estimations with greater errors because they did not account for acquisition  
8 dates. Despite this, they often appeared among the best results (Figures 6, 7 & 8). In our opinion, this was due to  
9 the temporal structure of the composite product. In a previous study (Testa et al. 2014), acquisition dates in  
10 chestnut woods in north-western Italy were found to be distributed around the middle of compositing periods, i.e.  
11 around their 8<sup>th</sup> and 9<sup>th</sup> day. In this work, we considered values from MOD13<sub>RAW</sub> TS (that did not account for  
12 acquisition dates) to be nominally placed on compositing periods' 8<sup>th</sup> days. This fact should not prevent any user  
13 from accounting for acquisition dates: if the global statistics presented in this work were similar among  
14 comparisons both accounting and not accounting for acquisition dates, errors could have been introduced at the  
15 single-plot scale and SOS and EOS estimations could have been affected (Testa et al. 2014). Because of this, we  
16 think the use of daily or composite date-corrected TS is more reliable (Hmimina et al. 2013).

## 17 **6 – Conclusions**

18 The aim of this work was to find the best way to estimate SOS and EOS on deciduous, temperate forests. The  
19 fitting procedure we proposed here did not require the user to give an exact initialization of SOS and EOS  
20 parameters but only a reasonable time search window.

21 In general, we would suggest the use of composite TS since they allowed us to achieve results somewhat better  
22 than daily TS, and were easier and faster to manage.

23 Despite VI/TS combinations based on raw MOD13Q1 VIs (MOD13<sub>RAW</sub> TS) often led to well ranked results, the  
24 use of date-corrected TS is highly recommended. We suggest the use of temporally aligned TS as described in  
25 Testa et al. (2014) since such a procedure, in this study, led to the best results in estimating both SOS and early  
26 EOS and was formally correct since it accounted for acquisition dates.

27 Referring to MOD13<sub>ALIGNED</sub> TS, the use of NDVI would allow unbiased SOS estimation with a 12 day precision;  
28 the use of WDRVI<sub>0.20</sub> increased SOS estimations' precision to 10 days, but estimates were postponed by 3 days on

1 average. With regard to EOS, early yellowing was conveniently estimated by  $WDRVI_{0.05}$  with a delay of 2 days  
2 and average error of 23 days

3  $WDRVI_{0.20}$  performed similarly to EVI in estimating the advanced greening of canopies and  $WDRVI_{0.05}$   
4 performed similarly to EVI in estimating canopies yellowing. Because of this, despite further investigations are  
5 needed, WDRVI could possibly be considered as an additional “continuity” index, together with NDVI, to the  
6 AVHRR dataset, since it does not require the blue band.

7

## 8 **7 – Acknowledgements**

9 We are sincerely grateful to the editor and the reviewers for their thorough and helpful comments and suggestions  
10 that were usefully implemented to improve this work. Acknowledgments are due to the University of Idaho  
11 (Moscow, ID, United States) for the supplies made available in support of this work. MODIS imagery was  
12 obtained through the online Data Pool at the NASA Land Processes Distributed Active Archive Center (LP  
13 DAAC), USGS/Earth Resources Observation and Science (EROS) Center, Sioux Falls, South Dakota, USA  
14 ([https://lpdaac.usgs.gov/data\\_access](https://lpdaac.usgs.gov/data_access)).

15 We acknowledge the *Réseau National de suivi à long terme des ECOSystèmes FORestiers* (RENECOFOR) for the  
16 ground data they gently and quickly supplied, allowing us to compare our results to ground measurements.

17 We thank Prof. Maria Carla Tabò and Dr. Axel Furlan for their valuable technical and mathematical support to  
18 this research.

## 2 8 – Bibliography

- 3 Ahl, D.E., Gower, S.T., Burrows, S.N., Shabanov, N.V., Myneni, R.B., & Knyazikhin, Y. (2006). Monitoring spring  
4 canopy phenology of a deciduous broadleaf forest using MODIS. *Remote Sensing of Environment*, 104, 88-95
- 5 Atkinson, P.M., Jeganathan, C., Dash, J., & Atzberger, C. (2012). Inter-comparison of four models for smoothing  
6 satellite sensor time-series data to estimate vegetation phenology. *Remote Sensing of Environment*, 123, 400-417
- 7 Aubinet, M., Heinesch, B., & Longdoz, B. (2002). Estimation of the carbon sequestration by a heterogeneous forest:  
8 night flux corrections, heterogeneity of the site and inter-annual variability. *Global Change Biology*, 8, 1053-1071
- 9 Beaubien, E.G., & Hall-Beyer, M. (2003). Plant phenology in western Canada: Trends and links to the view from space.  
10 *Environmental Monitoring and Assessment*, 88, 419-429
- 11 Beck, P.S.A., Atzberger, C., Hogda, K.A., Johansen, B., & Skidmore, A.K. (2006). Improved monitoring of vegetation  
12 dynamics at very high latitudes: A new method using MODIS NDVI. *Remote Sensing of Environment*, 100, 321-334
- 13 Bequet, R., Campioli, M., Kint, V., Vansteenkiste, D., Muys, B., & Ceulemans, R. (2011). Leaf area index development  
14 in temperate oak and beech forests is driven by stand characteristics and weather conditions. *Trees-Structure and  
15 Function*, 25, 935-946
- 16 Bleiholder, H., van den Boom, T., Langeluddeke, P., & Stauss, R. (1989). Einheitliche Codierung der phanologischen  
17 Stadien bei Kultur- und Schadpflanzen. *Gesunde Pflanzen*, 41, 381-384
- 18 Bradley, B.A., Jacob, R.W., Hermance, J.F., & Mustard, J.F. (2007). A curve fitting procedure to derive inter-annual  
19 phenologies from time series of noisy satellite NDVI data. *Remote Sensing of Environment*, 106, 137-145
- 20 Bradley, N.L., Leopold, A.C., Ross, J., & Huffaker, W. (1999). Phenological changes reflect climate change in  
21 Wisconsin. *Proceedings of the National Academy of Sciences of the United States of America*, 96, 9701-9704
- 22 Breda, N., Granier, A., & Aussenac, G. (1995). Effects of thinning on soil and tree water relations, transpiration and  
23 growth in an oak forest (*Quercus-petraea* (Matt) Liebl). *Tree Physiology*, 15, 295-306
- 24 Brooke, M.d.L., Jones, P.J., Vickery, J.A., & Waldren, S. (1996). Seasonal Patterns of Leaf Growth and Loss,  
25 Flowering and Fruiting on a Subtropical Central Pacific Island. *Biotropica*, 28, 164-179
- 26 Brügger, R., Dobbertin, M., & Krauchi, N. (2003). Phenological variation of forest trees. *Phenology: an Integrative  
27 Environmental Science*, 39, 255-267
- 28 Colombo, R., Busetto, L., Fava, F., Di Mauro, B., Migliavacca, M., Cremonese, E., Galvagno, M., Rossini, M., Meroni,  
29 M., Cogliati, S., Panigada, C., Siniscalco, C., & di Cella, U.M. (2011). Phenological monitoring of grassland and larch  
30 in the Alps from Terra and Aqua MODIS images. *Italian Journal of Remote Sensing-Rivista Italiana Di  
31 Telerilevamento*, 43, 83-96
- 32 Colombo, R., Busetto, L., Migliavacca, M., Cremonese, E., Meroni, M., Galvagno, M., Rossini, M., Siniscalco, C., & di  
33 Cella, U.M. (2009). On the spatial and temporal variability of Larch phenological cycle in mountainous areas. *Rivista  
34 Italiana Di Telerilevamento*, 41, 79-96
- 35 Cowie, J. (2007). *Climate Change: Biological and Human Aspects*. Cambridge: Cambridge University Press
- 36 Crucifix, M., Betts, R.A., & Cox, P.M. (2005). Vegetation and climate variability: a GCM modelling study. *Climate  
37 Dynamics*, 24, 457-467
- 38 Davi, H., Soudani, K., Deckx, T., Dufrene, E., Le Dantec, V., & Francois, C. (2006). Estimation of forest leaf area  
39 index from SPOT imagery using NDVI distribution over forest stands. *International Journal of Remote Sensing*, 27,  
40 885-902
- 41 de Beurs, K.M., Henebry, G.M. (2004). Land surface phenology, climatic variation, and institutional change: Analyzing  
42 agricultural land cover change in Kazakhstan, *Remote Sensing of Environment*, Volume 89, Issue 4, 29 February 2004,  
43 Pages 497-509, ISSN 0034-4257, <http://dx.doi.org/10.1016/j.rse.2003.11.006>.
- 44 de Beurs, K.M., & Henebry, G.M. (2005). A statistical framework for the analysis of long image time series.  
45 *International Journal of Remote Sensing*, 26, 1551-1573
- 46 de Beurs, K.M., & Henebry, G.M. (2010a). A land surface phenology assessment of the northern polar regions using  
47 MODIS reflectance time series. *Canadian Journal of Remote Sensing*, 36, S87-S110
- 48 de Beurs, K.M., & Henebry, G.M. (2010b). Spatio-Temporal Statistical Methods for Modelling Land Surface  
49 Phenology. *Phenological Research: Methods for Environmental and Climate Change Analysis*, 177-208
- 50 Defila, C. (1992). Phenology, an indicator for environmental changes. *Schweizerische Rundschau fur Medizin Praxis =  
51 Revue suisse de medecine Praxis*, 81, 343-346
- 52 Delpierre, N.; Vitasse, Y. ; Chuine, I. ; Guillemot, J. ; Bazot, S. ; Rutishauser, T. & Rathgeber C.K. (2015). Temperate  
53 and boreal forest tree phenology: from organ-scale processes to terrestrial ecosystem models. *Annals of Forest Sciences*,  
54 1-21. 10.1007/s13595-015-0477-6
- 55 Delpierre, N.; Dufrene, E.; Soudani, K.; Ulrich, E.; Cecchini, S.; Boé, J. & François, C. (2009). Modelling interannual  
56 and spatial variability of leaf senescence for three deciduous tree species in France. *Agricultural and Forest  
57 Meteorology*, 149, 938-948

- 1 Demarée, G.R., & Rutishauser, T. (2009). Origins of the Word “Phenology”. *Eos, Transactions American Geophysical*  
2 *Union, 90*, 1
- 3 Eklundh, L., Johansson T., & Solberg S. (2009). Mapping insect defoliation in Scots pine with MODIS time-series data.  
4 *Remote Sensing of Environment, 113*, 1566-1573
- 5 Elmore, A. J., Guinn, S. M., Minsley, B. J., & Richardson, A. D. (2012). Landscape controls on the timing of spring,  
6 autumn, and growing season length in mid-Atlantic forests. *Global Change Biology, 18*, 656–674.
- 7 Elzinga, J.A., Atlan, A., Biere, A., Gigord, L., Weis, A.E., & Bernasconi, G. (2007). Time after time: flowering  
8 phenology and biotic interactions. *Trends in Ecology & Evolution, 22*, 432-439
- 9 European Environment Agency (2004). Impacts of Europe’s changing climate. In, *An indicator based assessment*.
- 10 European Environment Agency (2012). Climate change, impacts and vulnerability in Europe 2012. In, *An indicator-*  
11 *based report*
- 12 Fabian, P., & Menzel, A. (1998). Changes in phenology of trees in Europe. In, *International Seminar on Causes and*  
13 *Consequences of Accelerating Tree Growth in Europe* (pp. 43-51). Nancy, France
- 14 Fenner, M. (1998). The phenology of growth and reproduction in plants. *Perspectives in Plant Ecology, Evolution and*  
15 *Systematics, 1*, 78-91
- 16 Fisher, J.I., Mustard, J.F., & Vadeboncoeur, M.A. (2006). Green leaf phenology at Landsat resolution: Scaling from the  
17 field to the satellite. *Remote Sensing of Environment, 100*, 265-279
- 18 Ganguly, S., Friedl, M.A.; Tan, B.; Zhang, X. & Verma, V. (2014). Land surface phenology from MODIS:  
19 Characterization of the collection 5 global land cover dynamics product. *Remote Sensing of Environment, 114*, 1805-  
20 1816
- 21 Gitelson, A.A. (2004). Wide dynamic range vegetation index for remote quantification of biophysical characteristics of  
22 vegetation. *Journal of Plant Physiology, 161*, 165-173
- 23 Gond, V., de Pury, D.G.G., Veroustraete, F., & Ceulemans, R. (1999). Seasonal variations in leaf area index, leaf  
24 chlorophyll, and water content; scaling-up to estimate fAPAR and carbon balance in a multilayer, multispecies  
25 temperate forest. *Tree Physiology, 19*, 673-679
- 26 Granier, A., Ceschia, E., Damesin, C., Dufrene, E., Epron, D., Gross, P., Lebaube, S., Le Dantec, V., Le Goff, N.,  
27 Lemoine, D., Lucot, E., Ottorini, J.M., Pontailier, J.Y., & Saugier, B. (2000). The carbon balance of a young Beech  
28 forest. *Functional Ecology, 14*, 312-325
- 29 Gu, L.H., Post, W.M., Baldocchi, D., Black, T.A., Verma, S.B., Vesala, T., & Wofsy, S.C. (2003). Phenology of  
30 vegetation photosynthesis. *Phenology: an Integrative Environmental Science, 39*, 467-485
- 31 Gutman, G., Ignatov, A., & Olson, S. (1995). Global land monitoring using AVHRR time-series. *Calibration and*  
32 *Applications of Satellite Sensors for Environmental Monitoring, 17*, 51-54
- 33 Henebry GM. 2013. Phenologies of North American Grasslands and Grasses. In: (MD Schwartz, ed.) *Phenology: An*  
34 *Integrative Environmental Science, 2e*. Springer. Chapter 11, pp. 197-210.
- 35 Hird, J.N., & McDermid, G.J. (2009). Noise reduction of NDVI time series: An empirical comparison of selected  
36 techniques. *Remote Sensing of Environment, 113*, 248-258
- 37 Hmimina, G., Dufrene, E., Pontailier, J.Y., Delpierre, N., Aubinet, M., Caquet, B., de Grandcourt, A., Burban, B.,  
38 Flechard, C., Granier, A., Gross, P., Heinesch, B., Longdoz, B., Moureaux, C., Ourcival, J.M., Rambal, S., Saint Andre,  
39 L., & Soudani, K. (2013). Evaluation of the potential of MODIS satellite data to predict vegetation phenology in  
40 different biomes: An investigation using ground-based NDVI measurements. *Remote Sensing of Environment, 132*,  
41 145-158
- 42 Holben, B.N. (1986). Characteristics of maximum-value composite images from temporal AVHRR data. *International*  
43 *Journal of Remote Sensing, 7*, 1417-1434
- 44 Huete, A., Justice, C., & van Leeuwen, W. (1999). MODIS Vegetation Index (MOD13) Algorithm Theoretical Basis  
45 Document.
- 46 Hufkens, K., Friedl, M., Sonnentag, O., Braswell, B.H., Milliman, T., & Richardson, A.D. (2012). Linking near-surface  
47 and satellite remote sensing measurements of deciduous broadleaf forest phenology. *Remote Sensing of Environment,*  
48 *117*, 307-321
- 49 Jiang, Z., Huete, A.R., Didan, K., Miura, T., 2008. Development of a two-band enhanced vegetation index without  
50 a blue band. *Remote Sensing of Environment, 112*, 3833–3845.
- 51 Jönsson, P., & Eklundh, L. (2002). Seasonality extraction by function fitting to time-series of satellite sensor data. *Ieee*  
52 *Transactions on Geoscience and Remote Sensing, 40*, 1824-1832
- 53 Jönsson, P., & Eklundh, L. (2003). *Seasonality extraction from satellite sensor data*.
- 54 Jönsson, P., & Eklundh, L. (2004). TIMESAT - a program for analyzing time-series of satellite sensor data. *Computers*  
55 *& Geosciences, 30*, 833-845
- 56 Keatley, M.R., & Fletcher, T.D. (2003). Australia in Phenology: An Integrative Environmental Science. In K.A.p. M.D.  
57 Schwartz (Ed.) (pp. 27-44)

- 1 Koch, E., Bruns, E., Chmielewski, F.-M., Defila, C., Lipa, W., & Menzel, A. (2008). Guidelines for plant phenological  
2 observations. In: WMO Technical Commission for Climatology, Open Program Area Group on Monitoring and  
3 Analysis of Climate Variability and Change (OPAG2).
- 4 Liang, L., & Schwartz, M.D. (2009). Landscape phenology: an integrative approach to seasonal vegetation dynamics.  
5 *Landscape Ecology*, 24, 465-472
- 6 Liang, L., Schwartz, M.D., & Fei, S. (2011). Validating satellite phenology through intensive ground observation and  
7 landscape scaling in a mixed seasonal forest. *Remote Sensing of Environment*, 115, 143-157
- 8 Lieberman, D., & Milton, L. (1984). The Causes and Consequences of Synchronous Flushing in a Dry Tropical Forest.  
9 *Biotropica*, 16, 193-201
- 10 Lieth, H. (1974). *Phenology and Seasonality Modeling*. New York, N.Y., U.S.A.; Heidelberg, West Germany: Springer-  
11 Verlag
- 12 LP DAAC (2014). Surface Reflectance Daily L2G Global 1km and 500m - MOD09GA user guide [http://modis-  
14 sr.ltdri.org/guide/MOD09\\_UserGuide\\_v1\\_3.pdf](http://modis-<br/>13 sr.ltdri.org/guide/MOD09_UserGuide_v1_3.pdf).
- 15 Melass, E.K., Friedl, M.A., & Zhu Z. (2013). Detecting interannual variation in deciduous broadleaf forest phenology  
16 using Landsat TM/ETM+ data. *Remote Sensing of Environment*, 132, 176-185.
- 17 Menzel, A., & Fabian, P. (1999). Growing season extended in Europe. *Nature*, 397, 659-659
- 18 Morisette, J.T., Richardson, A.D., Knapp, A.K., Fisher, J.I., Graham, E.A., Abatzoglou, J., Wilson, B.E., Breshears,  
19 D.D., Henebry, G.M., Hanes, J.M., & Liang, L. (2009). Tracking the rhythm of the seasons in the face of global change:  
20 phenological research in the 21st century. *Frontiers in Ecology and the Environment*, 7, 253-260
- 21 Morren, C. (1849). *Le Globe, le Temps et la Vie*.
- 22 Nagler, P.L., Daughtry, C.S.T., & Goward, S.N. (2000). Plant litter and soil reflectance. *Remote Sensing of  
23 Environment*, 71, 207-215
- 24 Noormets, A. (2009). Phenology of Ecosystem Processes: Applications in Global Change Research. *Phenology of  
25 Ecosystem Processes: Applications in Global Change Research*
- 26 Nordli, O., Wielgolaski, F.E., Bakken, A.K., Hjeltnes, S.H., Mage, F., Sivle, A., & Skre, O. (2008). Regional trends for  
27 bud burst and flowering of woody plants in Norway as related to climate change. *International Journal of  
28 Biometeorology*, 52, 625-639
- 29 Office National des Forêts 2015. Welcome to the RENECOFOR Website. [www.onf.fr/renecofor/@@index.html](http://www.onf.fr/renecofor/@@index.html)
- 30 Parmesan, C., & Galbraith, H. (2004). Observed impacts of global climate change in the US. In (p. 56). Arlingtonk, VA:  
31 Pew Center on Global Climate Change
- 32 Penuelas, J., & Filella, I. (2001). Phenology - Responses to a warming world. *Science*, 294, 793-+
- 33 Penuelas, J., Rutishauser, T., & Filella, I. (2009). Phenology Feedbacks on Climate Change. *Science*, 324, 887-888
- 34 Ratkowsky, D.A. (1983). *Nonlinear regression modeling—A unified practical approach*.
- 35 Richardson, A.D., Bailey, A.S., Denny, E.G., Martin, C.W., & O'Keefe, J. (2006). Phenology of a northern hardwood  
36 forest canopy. *Global Change Biology*, 12, 1174-1188
- 37 Richardson, A.D., Keenan, T.F., Migliavacca, M., Ryu, Y., Sonnentag, O., & Toomey, M. (2013). Climate change,  
38 phenology, and phenological control of vegetation feedbacks to the climate system. *Agricultural and Forest  
39 Meteorology*, 169, 156-173
- 40 Rodriguez-Galiano, V.F., Dash, J., & Atkinson, P.M. (2015). Intercomparison of satellite sensor land surface phenology  
41 and ground phenology in Europe. *Geophysical Research Letters*, 42, 2253-2260
- 42 Rosenzweig, C., Casassa, G., Karoly, D.J., Imeson, A., Liu, C., Menzel, A., Rawlins, S., Root, T.L., Seguin, B., &  
43 Tryjanowski, P. (2007). Assessment of observed changes and responses in natural and managed systems. *Climate  
44 Change 2007: Impacts, Adaptation and Vulnerability. Contribution of Working Group II to the Fourth Assessment  
45 Report of the Intergovernmental Panel on Climate Change*. (pp. 79–131). Cambridge, UK: Cambridge UP
- 46 Ruml, M., & Vulić, T. (2005). Importance of phenological observations and predictions in agriculture. *Journal of  
47 Agricultural Sciences, Vol. 50, No 2*, 217-225
- 48 Sarvas, R. (1972). Investigations on the annual cycle of development of forest trees I. Autumn dormancy and winter  
49 dormancy. *Communicationes Instituti Forestalis Fenniae.*, 76
- 50 Sarvas, R. (1974). Investigations on the annual cycle of development of forest trees II. Active period. *Communicationes  
51 Instituti Forestalis Fenniae.*, 84
- 52 Schaber, J., & Badeck, F.-W. (2005). Plant phenology in Germany over the 20th century. *Regional Environmental  
53 Change*, 5, 37-46
- 54 Schwartz, M.D. (1998). Green-wave phenology. *Nature*, 394, 839-840
- 55 Sesnie, S.E., Dickson, B.G., Rosenstock, S.S., & Rundall, J.M. (2012). A comparison of Landsat TM and MODIS  
56 vegetation indices for estimating forage phenology in desert bighorn sheep (*Ovis canadensis nelsoni*) habitat in the  
57 Sonoran Desert, USA. *International Journal of Remote Sensing*, 33, 276-286
- 58 Setiawan, Y., Yoshino, K., & Prasetyo, L.B. (2014). Characterizing the dynamics change of vegetation cover on  
59 tropical forestlands using 250 m multi-temporal MODIS EVI. *International Journal of Applied Earth Observation and  
60 Geoinformation*, 26, 132-144

1 Solano, R., Didan, K., Jacobson, A., & Huete, A. (2010). MODIS Vegetation Index User's Guide (MOD13 Series).  
2 *Version 2.00, May 2010 (Collection 5):* Vegetation Index and Phenology Lab - The University of Arizona.  
3 [http://vip.arizona.edu/documents/MODIS/MODIS\\_VI\\_UsersGuide\\_01\\_2012.pdf](http://vip.arizona.edu/documents/MODIS/MODIS_VI_UsersGuide_01_2012.pdf)

4 Song, Y., Njoroge, J.B., & Morimoto, Y. (2013). Drought impact assessment from monitoring the seasonality of  
5 vegetation condition using long-term time-series satellite images: a case study of Mt. Kenya region. *Environmental*  
6 *Monitoring and Assessment, 185*, 4117-4124

7 Soudani, K., Francois, C., le Maire, G., Le Dantec, V., & Dufrene, E. (2006). Comparative analysis of IKONOS, SPOT,  
8 and ETM+ data for leaf area index estimation in temperate coniferous and deciduous forest stands. *Remote Sensing of*  
9 *Environment, 102*, 161-175

10 Soudani, K., Hmimina, G., Delpierre, N., Pontailier, J.Y., Aubinet, M., Bonal, D., Caquet, B., de Grandcourt, A.,  
11 Burban, B., Flechard, C., Guyon, D., Granier, A., Gross, P., Heinesh, B., Longdoz, B., Loustau, D., Moureaux, C.,  
12 Ourcival, J.M., Rambal, S., Saint Andre, L., & Dufrene, E. (2012). Ground-based Network of NDVI measurements for  
13 tracking temporal dynamics of canopy structure and vegetation phenology in different biomes. *Remote Sensing of*  
14 *Environment, 123*, 234-245

15 Soudani, K., le Maire, G., Dufrene, E., Francois, C., Delpierre, N., Ulrich, E., & Cecchini, S. (2008). Evaluation of the  
16 onset of green-up in temperate deciduous broadleaf forests derived from Moderate Resolution Imaging  
17 Spectroradiometer (MODIS) data. *Remote Sensing of Environment, 112*, 2643-2655

18 Studer, S., Stockli, R., Appenzeller, C., & Vidale, P.L. (2007). A comparative study of satellite and ground-based  
19 phenology. *International Journal of Biometeorology, 51*, 405-414

20 Testa, S., Mondino, E.C.B., & Pedroli, C. (2014). Correcting MODIS 16-day composite NDVI time-series with actual  
21 acquisition dates. *European Journal of Remote Sensing, 47*, 285-305

22 Thayn, J.B., & Price, K.P. (2008). Julian dates and introduced temporal error in remote sensing vegetation phenology  
23 studies. *International Journal of Remote Sensing, 29*, 6045-6049

24 Thomas, K.A., Denny, E.G., Miller-Rushing, A.J., Crimmins, T.M., & Weltzin, J.F. (2010). The National Phenology  
25 Monitoring System v0.1. In, *USA-NPN Technical Series 2010-001*

26 Tucker, Compton J. (1979). Red and photographic infrared linear combinations for monitoring vegetation. *Remote*  
27 *sensing of Environment, 8*, 2, 127-150, 1979, Elsevier

28 vanLeeuwen, W.J.D., & Huete, A.R. (1996). Effects of standing litter on the biophysical interpretation of plant canopies  
29 with spectral indices. *Remote Sensing of Environment, 55*, 123-138

30 Villegas, D., Aparicio, N., Blanco, R., & Royo, C. (2001). Biomass accumulation and main stem elongation of durum  
31 wheat grown under Mediterranean conditions. *Annals of Botany, 88*, 617-627

32 Vitasse, Y., & Basler, D. (2013). What role for photoperiod in the bud burst phenology of European beech. *European*  
33 *Journal of Forest Research, 132*, 1-8

34 Viña, A., & Gitelson, A.A. (2005). New developments in the remote estimation of the fraction of absorbed  
35 photosynthetically active radiation in crops. *Geophysical Research Letters, 32*, 4

36 Wolfe, R.E., Roy, D.P., & Vermote, E. (1998). MODIS land data storage, gridding, and compositing methodology:  
37 Level 2 grid. *Ieee Transactions on Geoscience and Remote Sensing, 36*, 1324-1338

38 World Meteorological Organization (2006). Systematic observation requirements for satellite-based products for  
39 climate. In U.n.e. programme, & I.c.f. science (Eds.), *Supplemental details to the satellite-based component of the*  
40 *"Implementation Plan for the Global Observing System for Climate in Support of the UNFCCC"*

41 Xiao, X.M., Braswell, B., Zhang, Q.Y., Boles, S., Frohling, S., & Moore, B. (2003). Sensitivity of vegetation indices to  
42 atmospheric aerosols: continental-scale observations in Northern Asia. *Remote Sensing of Environment, 84*, 385-392

43 Zhang, X.; Friedl, M.A. & Schaaf, C.B. (2006). Global vegetation phenology from Moderate Resolution Imaging  
44 Spectroradiometer (MODIS): Evaluation of global patterns and comparison with in situ measurements. *Journal of*  
45 *Geophysical Research, 111*, G04017, doi:10.1029/2006JG000217.

46 Zhang, X., Friedl, M.A., & Schaaf, C.B. (2009). Sensitivity of vegetation phenology detection to the temporal  
47 resolution of satellite data. *International Journal of Remote Sensing, 30*, 2061-2074

48 Zhang, X.Y., Friedl, M.A., Schaaf, C.B., Strahler, A.H., Hodges, J.C.F., Gao, F., Reed, B.C., & Huete, A. (2003).  
49 Monitoring vegetation phenology using MODIS. *Remote Sensing of Environment, 84*, 471-475